Proceedings of ASME Turbo Expo 2011
GT2011
June 6-10, 2011, Vancouver, British Columbia, Canada

GT2011-45635

MODELLING OF AN AERO ENGINE BEARING CHAMBER USING ENHANCED CFD TECHNIQUE

Davide Peduto, Amir A. Hashmi,
Klaus Dullenkopf, Hans-Jörg Bauer
Institut für Thermische Strömungsmaschinen
Karlsruhe Institute of Technology
76128 Karlsruhe, Germany
Email:Davide.Peduto@kit.edu

Herve Morvan
UTC for Gas Turbine Transmission Systems
University of Nottingham
NG7 2RD, UK

ABSTRACT

This manuscript presents the application of an improved CFD methodology to simulate the scavenge system film flow phenomena in a real aero engine bearing chamber environment i.e. influence of seals and rotational shaft. Near the scavenge off-take, the usual thin film approach is not valid due to the occurrence of relative thick films (up to 5mm, comp. [1]) where film internal dynamics become very important. Therefore, other multiphase modelling techniques need to be explored. Young and Chew suggest in [2] that the Volume Of Fluid (VOF) method is the most suitable technique for air/oil system applications. Hashmi et al. reported in [3] that this free surface method for shear driven thick wall films in the bearing chamber environment needs additional provisions for turbulence modelling.

Accordingly, a simple correction is made to the $k-\varepsilon$ RNG turbulence model to improve the simulation results. The improved CFD methodology is applied to an engine representative geometry and proves to be robust and computationally efficient. The test conditions in the simulation was chosen in a way to avoid any droplet stripping from the film surface. It is shown that the applied methodology together with the correction in the turbulence modelling prove to play a vital role for a good comparison with experimental data. After validation the simulation results are used to describe the flow phenomena which occur in the bearing chamber for the investigated condition.

The introduced CFD modelling technique shows large potential for the development and trouble shooting purposes in the industrial environment.

INTRODUCTION

The oil system of an aero-engine lubricates and cools the gears and bearings. To ensure a high level of safety and reliability for many operating hours the oil system must be carefully designed. In order to avoid the commonly known failure causes like oil fire or oil coking in the bearing chambers detailed knowledge on the flow phenomena is essential as reported in [4].

The labyrinth used to seal the bearing chamber from the hot surroundings have to be pressurized by sealing air taken from the compressor bleeds. The fast moving shaft accelerates the air in the circumferential direction. On the other hand, a large volume of cooling and lubricating oil is ejected from the bearing as a film, ligaments or droplets, depending on the flow conditions around the bearing (comp. [5]), and enters the bearing chamber continuously. After being carried by the centrifugal forces to the outer wall of the bearing chamber the oil forms a wall film.

As a result of the air/oil interaction, a complex two-phase flow dominates the bearing chamber. Several experimental studies have been performed in the past and recently using simple and model bearing chamber test rigs to understand these complex two-phase flow phenomena. In the following a short overview summerizing some experimental investigations will be provided.

From the recent experimental analysis ([6], [7]) several interesting factors affecting the removal of oil through a generic scavenge system can be identified. The test rig is provided with a rotating shaft and a provision to test different scavenge off-take designs.

Liquid film enters the test rig concurrently means in direction of shaft rotation. The liquid flow rate, scavenge ratio and shaft rotational speed are varied and their influence on the sump residence volume and scavenge air/liquid discharge ratio was studied. Nevertheless, it has to be mentioned at this point that most of these investigations were carried out with simplified flow conditions e.g. low pressure level, a labyrinth seal was not present, vent off-take was abstracted with a hole exposed to atmospheric conditions in the test rig. Therefore, the transfer of knowledge to the real bearing chamber environment is debatable.

In [8], [9] and [10] a model bearing chamber test rig under more realistic boundary conditions was investigated and the authors found that the efficiency of scavenge system depends strongly on the vent off-take design, the sealing air and the shaft speed. For example, increasing chamber pressure adversely affects the oil removal from the scavenge line. Hence, oil is discharged via the vent off-take.

Based on available literature, some general rules can be established on the scavenge system design. For the low pressure bearing compartment, a deep sump design is found to be more appropriate since gravity is the main driving force. On the other hand, a shallow sump proves to be more efficient for the high pressure bearing chamber since high shear force distributes the oil film almost homogenously along the bearing chamber outer wall. However, no physically plausible explanations could be found for these rules. In addition to that, extension of their general applicability is ambiguous due to the fact that engine manufacturers are still facing some serious challenges designing an efficient and effective scavenge system. Therefore, the focus has now shifted to explore the potential of the state of the art multiphase modelling techniques available in the commercial CFD codes to systematically improve bearing chamber designs.

The major advantage lies in the fact that with the help of a CFD simulation, the complete flow field can be resolved and all the variables of interest can be studied in more detail. Therefore, the flow field can be understood and explained with confidence that can further lead to more general rules of scavenge design than at this time. The other advantages of using CFD as an alternative to full scale experimental investigations lies in the reducing of cost and time (e.g. during test rig construction, instrumentation etc.).

In the literature not only the experimental investigations, but also numerical investigations can be found. Due to the complexity of bearing chamber flow phenomena and the fact that the multiphase numerical techniques are still in the development phase, the numerical investigations are often restricted to highly simplified test cases. Since wall film flow (under the influence of shear & gravity forces) is one of the major features, attempts to resolve this flow regime is the topic of many recent and past publications. According to the important modelling features of shear driven wall film flow, modern CFD codes offer primarily two approaches, the all continuum full Euler-Euler approach and its derivative the Volume-Of-Fluid (VOF) homogenous modelling approach. Hashmi et al. investigated in [3] the available multiphase modelling techniques and suggest that the VOF method is the most suitable technique for shear driven thick wall films but needs additional provision for turbulence modelling. Other authors (e.g. [11] and [2]) have also shown that VOF has the potential to simulate wall film flow in bearing chamber environment.

In this paper, an engine representative geometry of a bearing chamber together with all the salient features like rotating shaft, labyrinth seal, scavenge pump was used to carryout the numerical experiments with a commercial CFD code. The corresponding experimental investigations were performed in the ITS model bearing chamber test rig at the Karlsuhe Institute of Technology (KIT). From the in-house experiments and literature data, it was found that in the upper half of the bearing chamber (near the vent) the circumferential distribution of the cooling oil film is usually a millimetre or less, whereas near the scavenge system the film thickness can be as high as 4 mm (comp. [1]). Therefore, for an interface tracking method like VOF, resolving the complete bearing chamber can mean prohibitly large number of cells in an industrial environment. To keep the number of cell in a limited range, a new methodology is adopted. With the help of open channel boundary condition, it was shown that the scavenge system can be sufficiently analyzed by simulating only the lower half of the bearing chamber. The introduced methodology can indirectly be used for the global analysis of the upper half of the bearing chamber. For example, the difference between the discharged air/oil through the scavenge off-take and the total oil flow inlet deliver indirectly the amount of air/oil that leaves the chamber via the vent line. Therefore the introduced methodology opens new opportunities for the bearing chamber modelling.

NOMENCLATURE

Symbol	Unit	Quantity
$\dot{V}$	$[l/h]$	Volume flow rate
u	$[m/s]$	Velocity
f	$[Hz]$	Frequency
t	$[s]$	Time
T	$[K]$	Temperature
C	$[F]$	Capacity
ε	$[F/m]$	Dielectricity
s	$[-]$	Height to width ratio
h	$[m]$	Height of chamber
b	$[m]$	Width of Chamber
d	$[m]$	Diameter
r	$[m]$	Radius
p	$[bar]$	Pressure
$\dot{m}$	$[kg/s]$	Mass flow rate
σ	$[N/m]$	Surface Tension

n	$[rpm]$	Rotational Speed
h^*	$[-]$	Non-dimensional film thickness
$h^*(t)$	$[-]$	Time dependent non dimensional film thickness
$\overline{h}$	$[m]$	Averaged film height
$\dot{m}^*$	$[-]$	Dimensionless discharged oil flow
$\overline{\dot{m}}$	$[kg/s]$	Time-averaged Mass flow rate

Subscripts

i	Inner radius (shaft)
a	Outer radius (chamber wall)
g	Gas phase
in	Inlet
$air, seal$	Sealing air flow
v	Vent
s	Scavenge
sh	Shaft
$total$	Air and oil
$pump$	Scavenge pump
$pipe$	Scavenge pipe
f	Film
$angle$	Angle in Chamber
max	Maximal

Abbreviations

UDF	User Defined Function
BC	Boundary conditions
VOF	Voulme of Fluid
FFT	Fast Fourier Transformation
SR	Scavenge ratio
CFL	Courant-Friedrichs-Lewy condition

EXPERIMENTAL INVESTIGATION

Experiments were performed for different rotational speeds using the high speed bearing chamber test rig of the Institut für Thermische Strömungsmaschinen at the KIT. A cross sectional view of the test rig is shown in figure 1. Only a brief description of the test facility is given in this manuscript. For further details other ITS publications e.g. [8] and [10] can be consulted. The rotor is supported by two bearings. A ball bearing is used to prevent axial and radial displacements of the rotor. Due to the small size of the ball bearing only a small amount of oil was supplied for lubrication. The second bearing is a squeeze film damped roller bearing.

Oil is supplied by an under race lubrication system $\dot{V}_{oil,max} = 400l/h$ at temperatures of $T_{oil,max} = 298K$. The roller bearing separates the two bearing chambers, where the oil is ejected after cooling and lubricating the bearing. Both chambers are sealed by air pressurized labyrinths. The sealing air was provided by a compressor with a maximum mass flow rate of $\dot{m}_{air,max} = 0.5kg/s$ and a temperature of $T_{air,max} = 298K$. The occurring complex two phase air/oil flow is discharged at the top and bottom of each chamber by a radial vent and scavenge off-take, respectively. Then the oil is separated from the air and returned into the tank. The vent and scavenge ports of each design were positioned in the center of the chamber as shown in figure 3 and were flush mounted with the outer radial housing of the chambers.

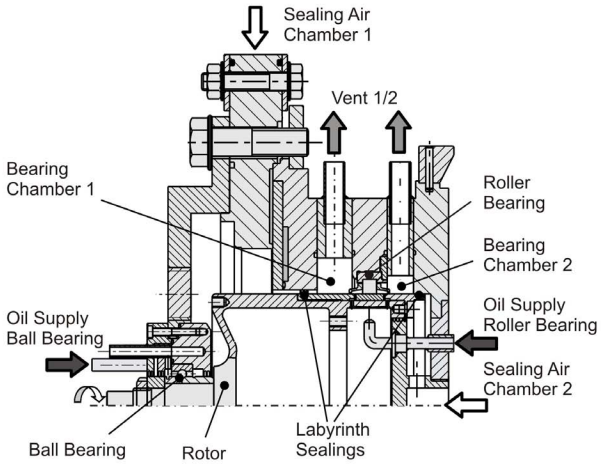

Figure 1. Co-axial section of high speed bearing chamber test rig (see [8])

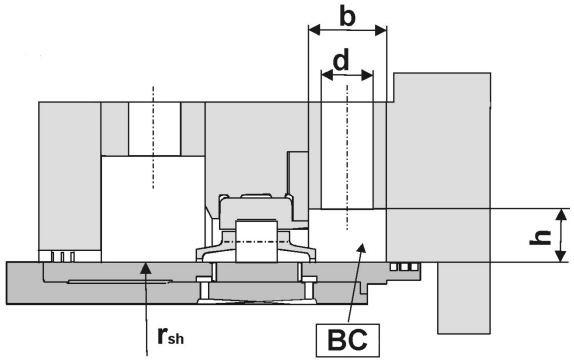

Figure 2. Dimensions of bearing chamber [8]

In figure 2, the geometry of the two bearing chambers in the test rig is shown in detail. The dimensions are provided in table 1. The experimental investigations were carried out in the bearing chamber number 2 (comp. figure 1). The bearing chamber is equipped with 10 capacitive sensors, circumferentially distributed at 30° intervals (comp. figure 3), for film thickness determination. Due to the small width of the chamber the axial film thickness is not resolved. The employed capacitive sensors have a diameter of 10 mm and give the mean film thickness over the sensor area. A detailed explanation of the measurement technique applied in the present investigation can be found in [8]. As mentioned earlier in this paper, as a first step towards engine representative bearing chamber conditions only the film flow i.e. no droplet stripping was considered. Accordingly, the boundary conditions set in the test rig are such to avoid the generation of droplets for example stripped from the film flow by high shear forces. The boundary conditions are summarized in table 1, too.

Height to width ratio	$r = h/b[-]$	0.066
Diameter of vent port	$d_v[m]$	0.01
Diameter of scavenge port	$d_s[m]$	0.01
Radius of rotor	$r_{sh}[m]$	0.064
Chamber pressure	$p_i[bar]$	ambient
Type of oil	Engine oil	Mobil Jet II
Air temperature	$T_{air,in}[K]$	298
Oil temperature	$T_{oil,in}[K]$	298
Sealing air-flow	$\dot{m}_{air,seal}[kg/s]$	0.003
Lubrication oil-flow	$\dot{m_{oil,in}}[kg/s]$	0.04
Surface Tension of oil	$\sigma_l[N/m]$	0.03008
Rotational Speed	$n[rpm]$	3500

Table 1. Bearing chamber dimensions, fluid properties and test conditions

The characteristic non-dimensional quantities for the verification and validation procedure are defined as follows. The scavenge ratio is a dimensionless number which describes the efficiency of a scavenge system in aero engine bearing chambers. In aero engine the SR is defined as follows,

$$SR = \frac{\dot{V}_{total,pump}}{\dot{V}_{oil,in}} \tag{1}$$

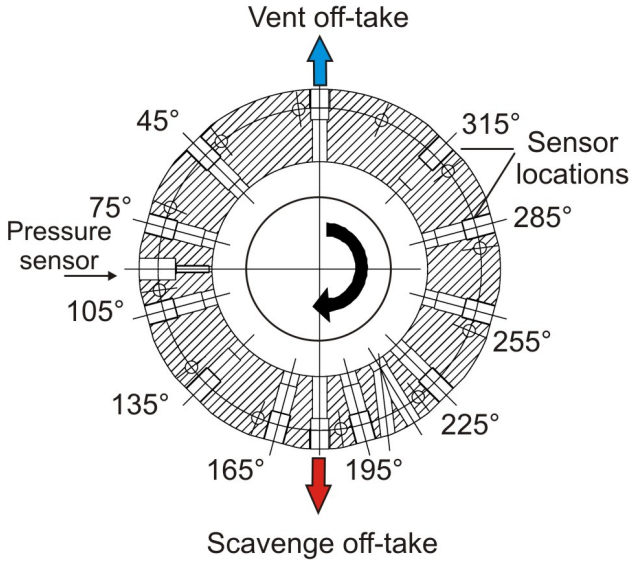

Figure 3. Cross section of bearing chamber with probe locations

The measured film thickness values inside the chamber are non-dimensionalized with the maximum film thickness experimentally achieved in the bearing chamber.

$$h^*_{f,angle} = \frac{\bar{h}_{f,angle,CFD}}{\bar{h}_{f,max,EXP}} \tag{2}$$

For comparison in the verification and validation procedure the calculated global discharged air/oil flow through the scavenge off-take is nondimensionalized with the experimentally measured oil flow rate.

$$\dot{m}^*_{air/oil} = \frac{\bar{\dot{m}}_{air/oil,pipe,CFD}}{\dot{m}_{oil,pipe,EXP}} \tag{3}$$

NUMERICAL INVESTIGATION

Mathematical model: To resolve the characteristic liquid film in the lower half of the bearing chamber (scavenge area) a homogenous Eulerian approach, the Volume of Fluid method (VOF), is employed. A good theoretical background of the method can be found in [12]. A geometric reconstruction scheme is used for the interface tracking. The scheme is based on a piecewise-linear approach (PLIC) developed by Rider and Kothe in [13]. To account for the surface tension effects, a continuum surface model (CSF) proposed by Brackbill et al. in [14] is employed. Due to the possibility of dry patches in the counter current flow regime, wall adhesion effects are also taken into account.

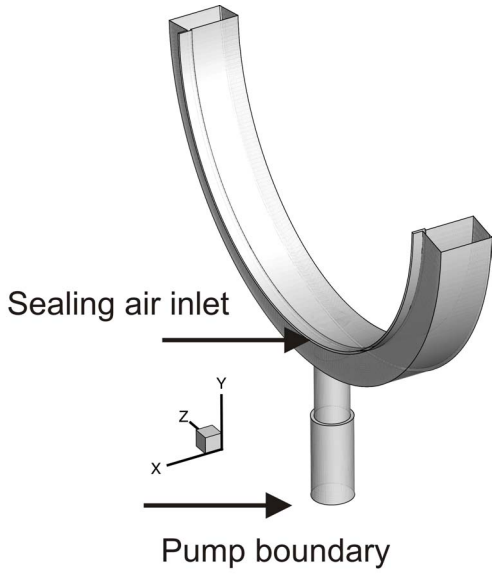

Figure 4. 3D model of the investigated bearing chamber

Numerical Setup: All computations are performed using a cell-centre-based finite volume method on a block structured structural grid. The CFD domain consists of the lower half of the bearing chamber number 2 as shown in figure 1. The solution procedure is based on the pressure implicit with splitting of operators (PISO) algorithm for pressure and velocity coupling in transient flows. The momentum transport equation is discretized with a second order Upwind method. The temporal discretization is carried out via the explicit first order backward difference method. Second order accuracy for the temporal discretization cannot be achieved due to the use of a geometric reconstruction scheme for the interface and an adaptive time step control which both require explicit first order accuracy. The adaptive time step is adjusted at the beginning of every time iteration loop to give a global CFL of 1-2. A detailed description of this methods is also presented in [15].

Boundary Conditions: The applied boundary conditions are summarized in table 2 and figures 5-6. Since only half of the bearing chamber is simulated, the boundary surfaces 1 and 2 in figure 5 act as inlets and outlets simultaneously. This means that depending on the flow field which establishes with the help of other boundary conditions as 3, 4, 6 & 7, a suitable mass flow of both phases independent of each other can either enter or exit the surfaces 1 & 2 at the same time. This is achieved with the help of total pressure boundary condition combined with the open channel option. This boundary condition requires the knowledge of film thickness which is provided from the experimental measurements. The scavenge pump was simulated according to [16].

	Boundary type	Required parameter
1	Open Channel Total Pressure	$h^*_{f,135} = 0.64$
2	Open Channel Total Pressure	$h^*_{f,255} = 0.46$
3	Mass-flow with $SR = 4$	$\dot{m}_{total,pump} = 4\dot{m}_{oil,in}$
4	Shaft	$n = 3500rpm$
5	Chamber Wall	Wall
6	Mass-flow inlet	Oil inlet swirl 45°
7	Mass-flow inlet	Air inlet swirl 45°

Table 2. Specification of boundary conditions

The end of the scavenge line is provided with a cylinder filled with oil and started draining at constant mass flow (surface 3 in figure 5) at the beginning of the simulation time. The volume of the cylinder was such to keep the pumping effect throughout the simulation i.e. until a quasi stationary state was achieved in the chamber. The test case was investigated with a scavenge ratio (SR) of 4. The rotating shaft (surface 4 in figures 5, 6) is defined as a moving wall with a rotational speed of $3500rpm$. The oil enters the domain via the side wall (surface 6 in figure 6) of the chamber with an assumed height and an inlet swirl of 45° in direction of shaft rotation, modelling the oil coming from a roller bearing. Gorse et al. [5] showed in his experiments that almost no droplets are produced at the roller bearing apart a strong cross flow of air through the bearing was introduced. Therefore, introducing the oil as a film should not limit the accuracy of the simulation. Furthermore, several simulations revealed that as long as the boundary film height is smaller then the film thickness in the chamber and the inlet swirl ranges between 0° & 45° in direction of shaft rotation no influence of the boundary condition on the flow field was found.

Sealing air is introduced in the domain via the labyrinth duct (surface 7 in fig. 6). The velocity profile at the sealing air inlet was calculated separately in a 2D axisymmetric labyrinth seal model to ensure appropriate profiles. Here, an inlet swirl of about 45° in direction of shaft rotation was calculated with the labyrinth seal model. Schramm et al. showed in [17] that a 2D axisymmetric approach is accurate enough to resolve the flow field in similar labyrinth seals. It has to be mentioned that the inlet swirl of the sealing air has a large impact on the air flow in a bearing chamber. For example depending on the boundary inlet swirl the torodial vortices in the chamber can change in number and rotation. Therefore, correct sealing air inlet flow conditions are absolutely necessary for a detailed two-phase flow analysis inside a bearing chamber.

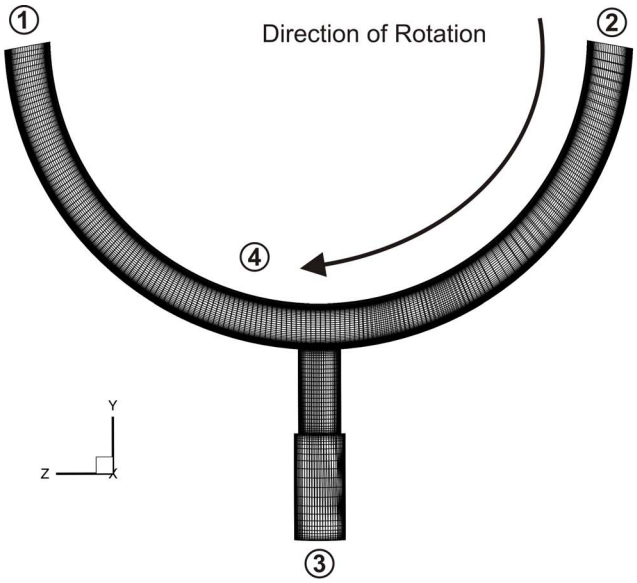

Figure 5. Model boundary bonditions 2 and mesh

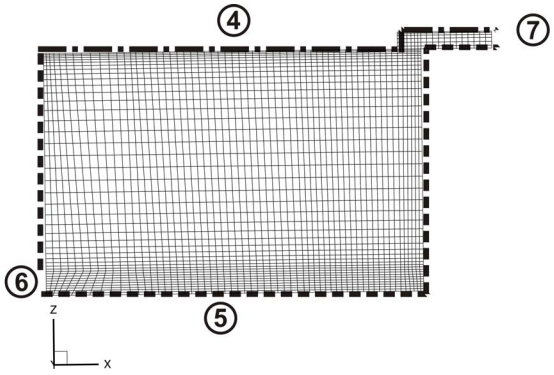

Figure 6. Model boundary bonditions 1 and mesh

Verification: For the verification of the methodology a test case with the presented conditions was prepared and summarized in table 1. Three different mesh densities (table 3) were used to test the fidelity of the introduced methodology. For all cases a simple interface treatment based on [3] was implemented and explained in the next section. The mesh was further refined in three stages where the interface between the wall film and the air was expected. It should be noted that for the denser meshes a decrease in time step was carried out to ensure solver stability.

The local time and area averaged film thickness at a circumferential position of 195° (comp. figure 3) and the global air/oil flow rate discharged through the off-take are analyzed in table 4. The resulting flow quantities are presented in the table 4. It can be seen from table 4 that further refinements from Mesh 1 to Mesh 3 has lead to discrepancies less than 8%.

Mesh	Total Number of Cells
1	506716
2	749028
3	1065342

Table 3. Size of applied meshes

Therefore, it can be said that the results achieved from the methodology are consistent and the number of element comprising Mesh 1 are high enough to resolve the investigated flow field.

Flow Quantity	Mesh 1	Mesh 2	Mesh 3
$h^*_{f,195°}$	0.69	0.74	0.72
$\dot{m}^*_{oil}$	0.91	0.94	0.93
$\dot{m}^*_{air}$	0.00728	0.00719	0.00715

Table 4. Mesh independency

Turbulence Modelling: The VOF method works perfectly for laminar cases but shows large discrepancies for turbulent cases ([3]). It was shown that the discrepancies arise from the homogenous modelling approach which allows additional (false) momentum transfer through turbulent stresses between the phases. However, the interface behaves like a wall and the turbulent stresses just adjacent to the interface must be zero. This general deficiency of the VOF method is due to the absence of interface (gas-liquid) physics in the model i.e. the two phase interface is though captured but has no physical meaning in the flow governing equations. This shortcoming in turbulence modelling leads to the fact that unphysical high turbulent viscosity is calculated near the interface as shown by Hashmi et al. in [3] and provided here in figure 7. The unphysical high turbulent viscosity near the interface has a global impact on the flow field and causes an unphysical gas side velocity profile (comp. figure 8). The latter citation contains a detailed analysis but to summerize it can be stated that for the original VOF simulation the momentum transfer at the interface is dominated by turbulent stresses. As a consequence the interface shear stress plays an insignificant role which disobeys the governing physics at the interface. For shear driven films, this also means that the momentum is transferred by a force (turbulent stress) acting on the complete volume instead of a surface (interface shear stress). This in turn has some serious consequences especially for resolving important flow structures e.g. recirculation regions in counter-current flows as will be discussed later.

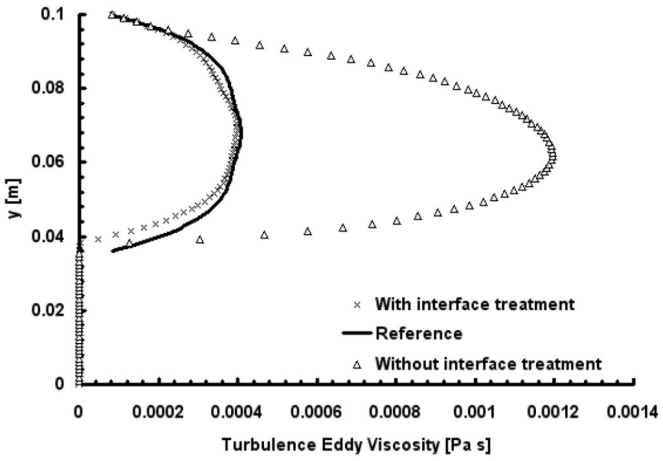

Figure 7. Turbulent viscosity with & without interface treatment in the channel test case from [3]

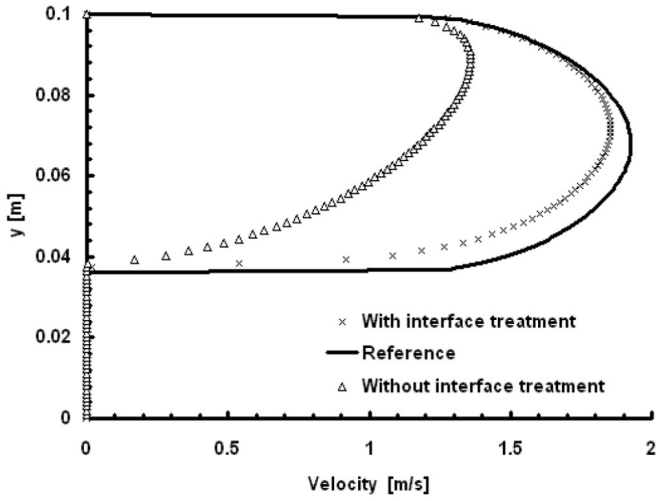

Figure 8. Velocity profile with & without interface treatment in the channel test case from [3]

For the turbulence cases, plausible results could only be obtained by defining suitable interface physics usually referred to as interface treatment in literature. In this paper, a simple interface treatment based on k-e turbulence model is combined with the introduced methodology to correct the turbulent quantities near the interface. This interface treatment identifies the cells where the interface is located and forces the turbulent viscosity in these cells to zero. For this purpose a UDF was written to implement in the CFD solver. This approach is primitive but used here because it is very easy to implement and serves the purpose of identifying the absolute need for interface treatment.

RESULTS AND DISCUSSION

A transient simulation was performed with an adaptive time step control as mentioned in the section describing the numerical investigation. The simulation was first started without rotating the shaft and sealing air until the liquid (oil) has reached the scavenge pipe (free draining). This tooks about 0.2s. The shaft is then rotated and the sealing air was introduced in the domain. The simulation was run until the flow field reaches quasi steady state. The test case is then validated against local and global measured quantities. After the validation, the flow aspects of the flow field are discussed with the help of CFD results.

Validation: In figure 9, the non dimensional film thickness at six angular positions are compared with experimental data. The film thicknesses to compare are averaged in time and with bearing chamber width and non dimensionalized with the maximum film thickness experimentally achieved. The film thickness distribution achieved from the VOF simulation without interface treatment shows large discrepancies to the experimental one. Especially from scavenge off-take downstream (in direction of shaft rotation) between $105 - 135°$, the film thickness decreases to nearly zero leading to dry patch in the simulation which was not observed in the experiment. From 165° onwards in the direction of the scavenge off-take and beyond, the film distribution is overestimated by the original VOF. For the investigated boundary conditions, VOF without interface treatment establishes only counter-current regime on both sides of the scavenge off-take. The rotating shaft enhances the air flow from $165 - 105°$ and reduces it from $195 - 225°$. Due to the high momentum transfer in the prediction without interface treatment a complete flow reversal occured between $105 - 135°$ where the air flow is accelarated. Hence, the occurrence of dry patch can be explained. Between $195 - 225°$ where a counter current flow establishes a local film thickening occures.

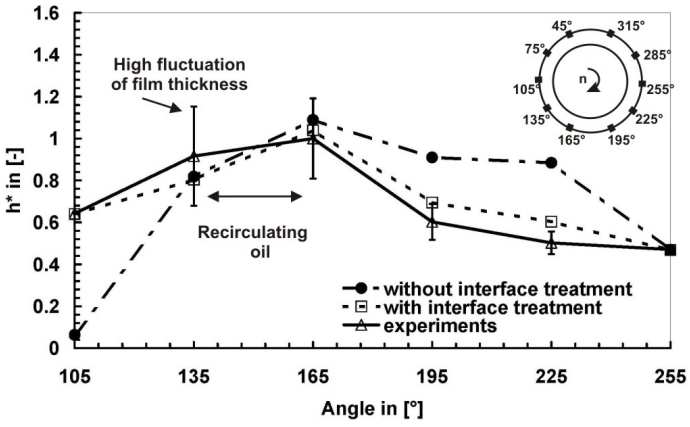

Figure 9. Comparison of angular film thickness distribution with and without interface treatment to the experimental data

On the other hand, the film thickness distribution achieved from the VOF prediction with interface treatment remains within $\pm 15\%$ of the measured mean film thickness. The film thickness was slightly underpredicted between $105-165^\circ$ and slightly overpredicted from 165° onwards. This as explained previously is a direct result of slight imperfection in the momentum transfer to the wall film hence points towards the need for further refinement in the interface treatment method applied in this study. This improved agreement between the calculated and the measured data can be attributed to minimizing the additional (false) momentum transfer to the wall film. As a result it automatically corrects the air velocity gradient of the interface as shown in figure 8 and considers that momentum is transferred by interface shear stress and not by turbulent stress. Moreover, as mentioned in the turbulence modelling section, the recirculation region can only be captured with interface treatment (see figure 10 (bottom)). It completely disappeared when calculated without interface treatment (see figure 10 (top)).

Besides capturing the recirculation region at all, it was also found that the occurrence of recirculation is a highly dynamic phenomenon which will be dealt with detail later in this paper. Generally the film surface remains flat for the case without interface treatment whereas other instabilities (waves) are also evident with interface treatment. In contrast to the case without interface treatment, where a complete dry out was predicted, no large dry out (only small points) could be found in the case with interface treatment.

In addition to the local film distribution, global quantities were compared, too. Table 5 shows the ratio of oil to the experimental measured oil discharged mass flow. As already described, original VOF results in considerably larger discrepancies than the enhanced VOF when compared to the real discharge flow. Without interface treatment, lower discharge oil mass flow from the scavenge pipe results from the unphysical large momentum transfer to the wall film. This can be understood by considering the fact that on either side of the off-take counter-current flow regime exists. Hence the air flow restricts the oil film entering the section at 105°. In the $180^\circ - 225^\circ$ sector the air flow holds the wall film in the process of thickening till gravitational force dominates and pulls the film towards the off-take (comp. figure 3 and [18] for further details on counter-current flow regime). It can be stated that the interface treatment minimizes the unphysical momentum transfer and the prediction of the oil discharge mass flow through the scavenge off-take is significantly improved.

Flow Quantity	without treatment	with treatment
$\dot{m}^*_{oil}$	0.8	0.91

Table 5. Global oil mass flow ratio discharged through the scavenge off-take: comparison of experiments, original VOF and enhanced VOF

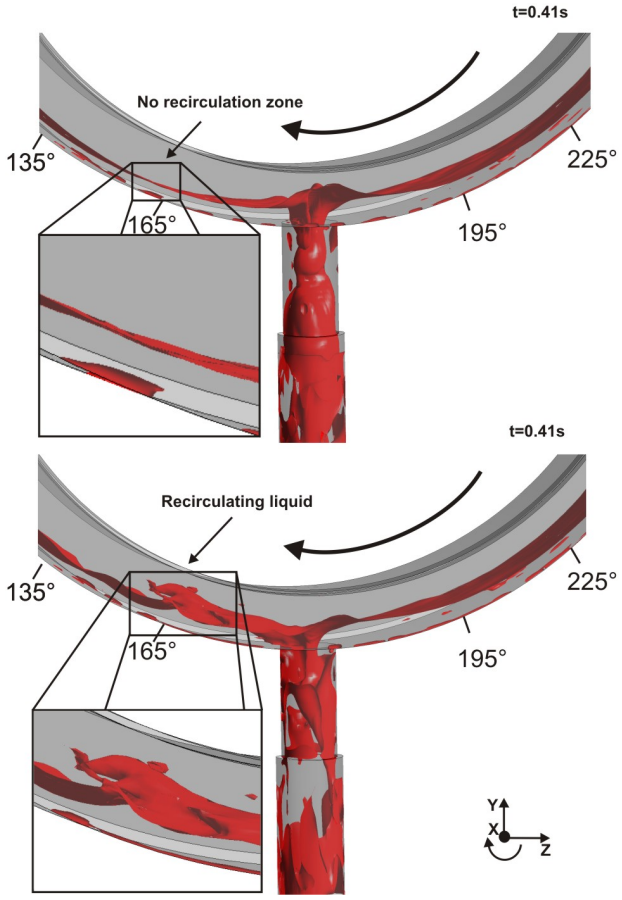

Figure 10. Comparison of oil volume fraction iso surface (50%) with (bottom) and without (top) interface treament

Flow field Analysis: In this section the flow phenomena as predicted by VOF simulation with interface treatment are discussed. As mentioned earlier, the recirculation zone could not only be resolved with the help of improved turbulence modelling but it was also found that the flow in this area is highly dynamic. This means that the recirculation zone cannot be localized to a certain position in time or space. Instead, it seems that as a result of interaction between the driving forces and off-take flow (geometry and scavenge ratio) it evolved at the off-take, carried away with the shearing air flow and in the process accumulating mass to a point where gravity balances the shear force. Simultaneously during the process of accumulating mass, the recirculation zone reduces the flow area for the sealing air hence build up huge resistance to the air flow that results in a split of the air flow.

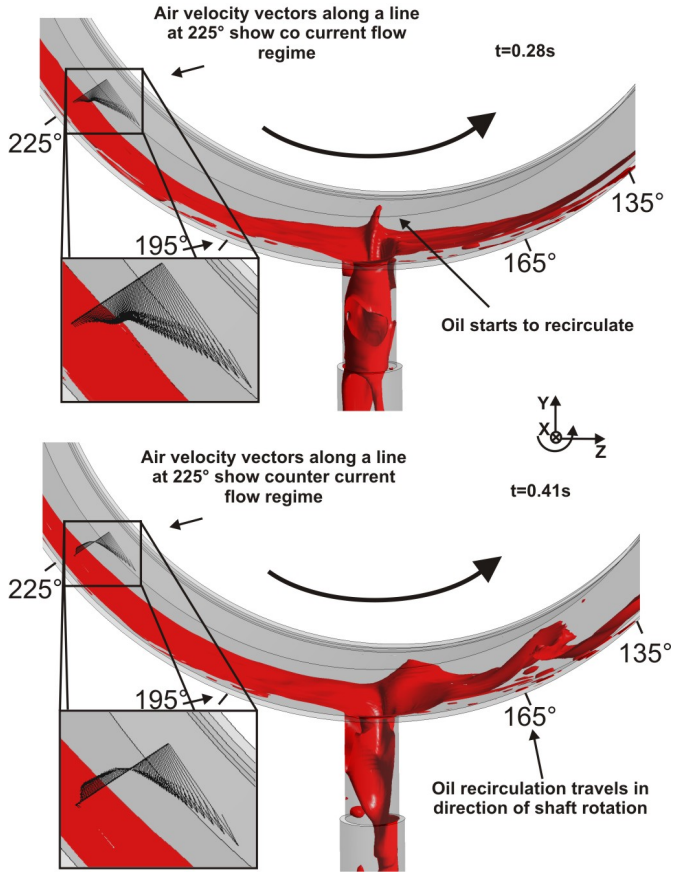

Figure 11. 50 % isosurface of oil volume fraction at $t = 0.28s$ (top) and $t = 0.41s$ (bottom) showing transition from co-current to counter current flow regime with time

A major part of air now flows in the opposite direction (see fig. 11 (bottom) at t=0.41s) whereas the rest still flows over the top of the recirculation zone and is accelerated. The top of the recirculating oil is teared off into large ligaments as a result of local acceleration until the recirculation region completely disappeared. This leads again to the reversal of air flow to the original direction and the flow now resembles state at previous time step (see figure 11 (top) at t=0.28s). From there onwards, the flow phenomenon repeats itself and it seems that its nature is periodic for the investigated conditions. Unfortunately, direct comparison to test data is not yet possible, however from the counter-current investigations in a bearing chamber environment in [18] the conclusion can be drawn that the dynamic behaviour of the recirculation zone explained here is physically plausible. The experiments in [18] were performed in a channel which was inclined to introduce gravitational force.

Increasing the counter acting air flow it was shown that big solitary waves of periodic nature form on the surface of liquid film which roll in the direction of air flow whereas a part of film still flows in the original direction i.e. opposite to air flow. With even further increase in the air flow, the solitary waves travel on the film surface with ligaments tearing off from the wave peaks as predicted by the CFD simulation presented.

To investigate this phenomenon in the experimental data, the raw film thickness signals were processed to look for evidence of periodicity. However it should be noted here that periodicity can only be captured if the frequency of periodicity is less than half the frequency of measuring equipment. Accordingly film thickness signals at all measured locations were investigated. Indeed periodic fluctuating signals were found for all locations as shown in figure 9. To further elaborate this fact, the raw signal of the non-dimensionalized film thickness is provided in figure 12 (top). The time trace of the signal already reveals a periodic nature of the signal. To further analyze the frequency content a FFT analysis of the signal was performed on the raw film thickness signal at 165° (comp. figure 12).

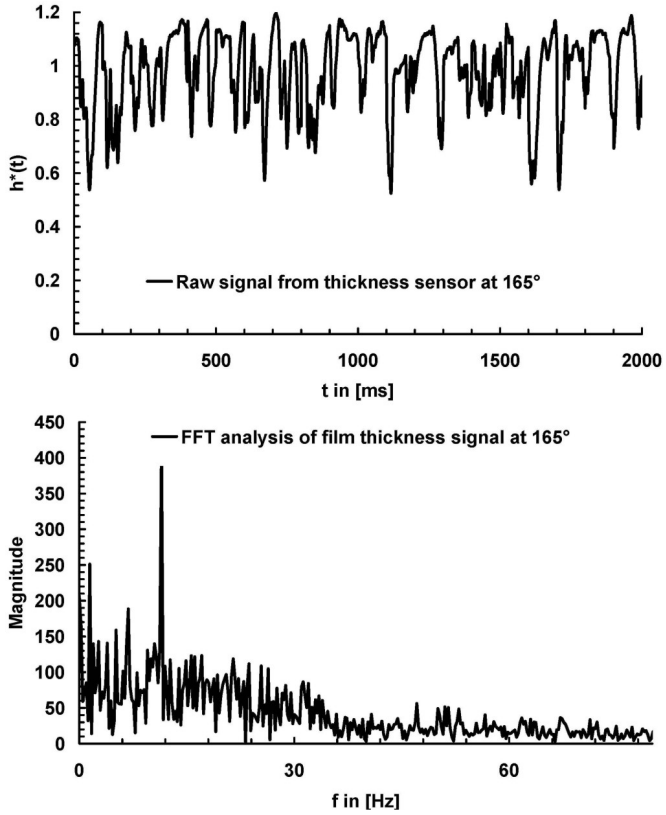

Figure 12. Raw signal of experimentally achieved non dimensional film thickness in time domain (top) and related frequency distribution (FFT) (bottom) at 165° in counter current regime

The result of the FFT is shown in the bottom of figure 12 where a dominant frequency of 11Hz can clearly be recognized. From the result of the FFT analysis it can again be stated that the prediction made by CFD is physically plausible. However, as mentioned before it is too early to state anything especially because the CFD simulation is only run only about 0.5s whereas the FFT shown in figure 12 (bottom) is performed on a data of two seconds.

The other important and interesting phenomenon predicted by the CFD simulation is the existence of strong secondary flows which can also be traced back to the experimental investigation of [8] in a similar bearing chamber geometry. CFD reports secondary flow with velocity up to 70% of the core velocity. This indicates the axial film thickness variation which can be seen in figure 13.

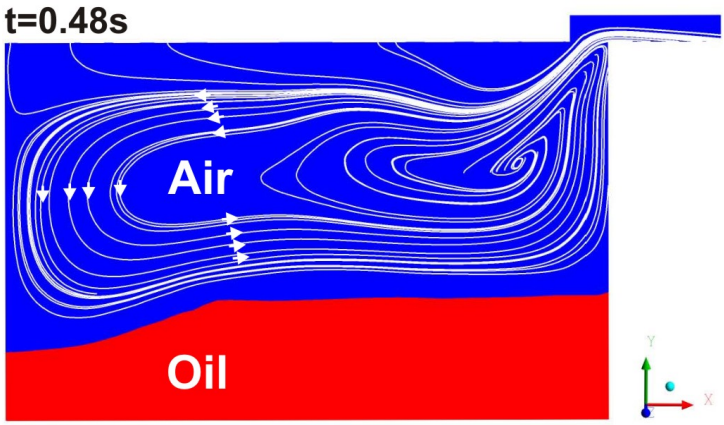

Figure 13. Contour plot of volume fraction with air in blue and oil in red and related air velocity streamlines at 165°)

Summerizing the results of the comparison it can be stated that VOF with appropriate interface treatment can be applied as a useful tool for the prediction of oil film flows affected by shear forces and gravity in a typical bearing chamber environment.

SUMMARY & OUTLOOK

In this paper a CFD methodology was described to simulate the thick wall film dynamics near the scavenge off-takes in a typical bearing chamber geometry. The methodology employs VOF method together with the total pressure open channel boundary condition to simulate the shear and gravity driven wall film flow in the lower half of the bearing chamber. The inherent problem of VOF method, i.e. additional (false) momentum transfer when dealing with turbulent flows, was solved by employing a simple interface treatment.

This interface treatment works by forcing the turbulent viscosity in the cells occupied by the interface to zero hence momentum is transferred by interface shear stress and not by turbulent stress. The simulated film thickness distribution was compared with experimental data. It was shown that the introduced methodology together with the interface treatment technique is able to reproduce experimentally obtained data for low pressure and shaft speeds.

In addition it was shown that the interface treatment is absolutely necessary for reproducing typical film surface instabilities e.g. waves, recirculation zone etc. which were completely absent in the case without interface treatment. The CFD results also showed that the recirculation zone is highly dynamic and probably periodic in nature which may influence the air flow by completely changing its direction. The periodicity of the flow phenomena in the experimentally investigated bearing chamber geometry can also be confirmed in the FFT analysis of the time dependent film thickness signal. Therefore the introduced methodology offers the potential for simulating multiphase flow phenomena at low pressure and shaft speeds. At high pressure and shaft speeds, the methodology can be extended with further modells i.e. droplet-wall film interaction etc. .

Furthermore this methodology can be coupled with an Euler-Euler method at the simultaneously acting inlets and outlets (surfaces 1 & 2) to exchange information so that the upper half of the bearing chamber can be involved. In this way the methodology introduced in this paper provides the option to simulate the complete bearing chamber.

ACKNOWLEDGEMENTS

The financial support from the German Federal Ministry of Economics and Technology and Rolls-Royce Deutschland within the cooperative research project 'Luftfahrtforschungsprogram 4 2010-2013 (20T0912C)' is highly appreciated. Furthermore, the authors would like to thank Rolls Royce UK for the sharing of experimental results. Special thanks also to Dr. Rainer Koch for sharing his experience in multiphase modelling techniques.

References

[1] Gorse, P., Busam, S., and Dullenkopf, K., 2004. "Influence of operating conditions and geometry on the oil film thickness in aero-engine bearing chambers". *ASME-Paper: GT2004-53708*.

[2] Young, C., and Chew, J., 2005. "Evaluation of the volume of fluid modelling approach for simulation of oil/air system flows". *ASME-paper: GT2005-68861*.

[3] Hashmi, A., Dullenkopf, K., Koch, R., and Bauer, H.-J., 2010. "CFD methods for shear driven liquid wall films". *ASME-Paper: GT2010-23532*.

[4] Willenborg, K., Busam, S., Rosskamp, H., and Wittig, S., 2002. "Experimental studies of the boundary conditions leading to the oil fire in the bearing chamber and in the secondary air system of aeroengines". *ASME-Paper: GT2002-30241*.

[5] Gorse, P., Dullenkopf, K., Bauer, H.-J., and Wittig, S., 2008. "An experimental study on droplet generation in bearing chambers caused by roller bearings". *ASME-Paper: GT2008-51281*.

[6] Chandra, B. W., 2006. "Flows in turbine engine oil sumps". Phd thesis, Purdue University West Lafayette, Indiana.

[7] Chandra, B., Pickering, S., Tittel, M., and Simmons, K., 2010. "Factors affecting oil removal from an aeroengine bearing chamber". *ASME-Paper: GT2010-22631*.

[8] Gorse, P., Willenborg, K., Busam, S., Ebner, J., and Dullenkopf, K., 2003. "3D-LDA measurements in an aeroengine bearing chamber". *ASME-Paper: GT2003-38376*.

[9] Busam, S., Glahn, A., and Wittig, S., 2000. "Internal bearing chamber wall heat transfer as a function of operating conditions and chamber geometry". *ASME, Journal of Engineering for Gas Turbines and Power,116*, pp. 395–401.

[10] Wittig, S., Glahn, A., and Himmelsbach, J., 1994. "Influence of high rotational speeds on heat transfer and oil film thickness in aero engine bearing chambers". *ASME Journal of Engineering for Gas Turbines and Power*, pp. 395–401.

[11] Robinson, A., Morvan, H., and Eastwick, C., 2010. "Further computational investigations into aero-engine bearing chamber off-take flows". *ASME-Paper: GT2010-22629*.

[12] Hirt, C. W., and Nichols, B. D., 1981. "Volume of fluid (vof) method for the dynamics of free boundaries". *Journal of Computer Science*, pp. 201–225.

[13] Rider, W. J., and Kothe, D., 1998. "Reconstructing volume tracking". *Journal of Computational Physics*, pp. 112–142.

[14] Brackbill, J. U., Kothe, D. B., and Zemach, C., 1992. "A continuum method for modeling surface tension". *Journal of Computer Science*, pp. 335–354.

[15] Ferziger, J., and Peric, M., 2003. *Computation of Fluid Dynamics*. Springer, Berlin, 3. Aufl.

[16] Robinson, A., Morvan, H., and Eastwick, C., 2011. "Simulating pumped oil off takes for bearing chamber applications". *ASME-Paper to be published at the ASME Turbo Expo 2011, Vancouver Canada*.

[17] Schramm, V., Denecke, J., Kim, S., and Wittig, S., 2004. "Shape optimization of a labyrinth seal applying the simulated annealing method". *International Journal of Rotating Machinery, Vol. 10*, pp. No. 5, Page 365–371.

[18] Hashmi, A., Dullenkopf, K., and Bauer, H.-J., 2011. "Experimental investigation of wall film dynamics in typical aero-engine bearing chamber geometry environment". *ASME-paper: GT 45545 to be published at the ASME Turbo Expo 2011 in Vancouver Canada*.